

# Dynamic modelling of CO<sub>2</sub> absorption for post combustion capture in coal-fired power plants

A. Lawal<sup>a</sup>, M. Wang<sup>a,\*</sup>, P. Stephenson<sup>b</sup>, H. Yeung<sup>a</sup>

<sup>a</sup>*Process Systems Engineering Group, School of Engineering, Cranfield University, Bedfordshire, MK43 0AL, UK.*

<sup>b</sup>*RWE npower, Windmill Park, Swindon, SN5 6PB, UK.*

---

## Abstract

Power generation from fossil fuel-fired power plants is the largest single source of CO<sub>2</sub> emissions. Post combustion capture via chemical absorption is viewed as the most mature CO<sub>2</sub> capture technique. This paper presents a study of the post-combustion CO<sub>2</sub> capture with monoethanolamine (MEA) based on dynamic modelling of the process. The aims of the project were to compare two different approaches (the equilibrium-based approach versus the rate-based approach) in modelling the absorber dynamically and to understand the dynamic behaviour of the absorber during part load operation and with disturbances from the stripper. A powerful modelling and simulation tool gPROMS was chosen to implement the proposed work. The study indicates that the rate-based model gives a better prediction of the chemical absorption process than the equilibrium-based model. The dynamic simulation of the absorber indicates normal absorber column operation could be maintained during part load operation by maintaining the ratio of the flow rates of the lean solvent and flue gas to the absorber. Disturbances in the CO<sub>2</sub> loading of the lean solvent to the absorber significantly affect absorber performance. Further work will extend the dynamic modelling to the stripper for whole plant analyses.

*Keywords:* CO<sub>2</sub> Capture, Chemical absorption, Dynamic modelling, Coal-fired power plant

---

## 1. Introduction

Power generation from fossil fuel-fired power plants is the largest single source of CO<sub>2</sub> emissions [1]. Coal-fired power plants release twice as much CO<sub>2</sub> per unit of electricity generated than natural gas power plants. However, these power plants play a vital role in meeting energy demands as coal is relatively cheap. In addition, coal-fired power plants can be operated flexibly as mid-merit plants in response to changes in supply and demand [2]. With growing concerns about the environmental impact of such plants effective CO<sub>2</sub> emission abatement strategies such as Carbon Capture and Storage (CCS) are required for their continued use. One approach to CCS is post combustion capture which involves the separation of CO<sub>2</sub> from the flue gas stream after combustion occurs (Figure 1). Chemical absorption is well suited for separating CO<sub>2</sub> from streams with low concentration of CO<sub>2</sub> (10-15% by volume) typical of pulverized fuel power plants [3,4].

### 1.1 Motivation

---

\* Corresponding author. Tel.: +0044 1234 754655; Fax: +0044 1234 754685; Email address: [meihong.wang@cranfield.ac.uk](mailto:meihong.wang@cranfield.ac.uk)

30 Several studies have shown that the energy requirement for solvent regeneration would have adverse effects on power plant  
31 efficiency [5-8]. These effects have been studied using various steady state models and techno-economic assessments.  
32 However there are several gaps in the understanding of the impact of post combustion capture on the operability of the  
33 power plant. For instance, would such power plants be able to effectively operate at varying loads? What modifications  
34 would have to be made to the conventional start-up and shutdown procedures? What implications would heat integration  
35 between the power plant and CO<sub>2</sub> capture facility have on their operation [9]? These questions can be addressed by  
36 studying the dynamic behaviour of such plants. To achieve this, accurate dynamic models of the power plant and the CO<sub>2</sub>  
37 capture facility are required.

### 38 *1.2. Post combustion capture via chemical absorption*

39 Chemical absorption involves the reaction of CO<sub>2</sub> with a chemical solvent to form a weakly bonded intermediate  
40 compound which may be regenerated with the application of heat producing the original solvent and a CO<sub>2</sub> stream [3,4].  
41 Monoethanolamine (MEA) being a primary amine reacts with CO<sub>2</sub> to produce carbamate via sets of liquid phase reactions  
42 [7,10]. A review of various reaction schemes describing this process is available in literature [11,12].

43 Figure 1 describes one of the popular technologies proposed for post combustion capture. The facility consists of two main  
44 units – the absorber and stripper columns which are both packed columns. Flue gas from the power plant is contacted  
45 counter-currently with lean MEA solution in the absorber. MEA chemically absorbs the CO<sub>2</sub> in the flue gas. This leaves a  
46 treated gas stream of much lower CO<sub>2</sub> content. The solvent solution (now Rich MEA) is regenerated in the stripper column  
47 using steam derived from the power generation process. CO<sub>2</sub> from the top of the column is compressed and transported  
48 away while the lean (regenerated) MEA solution is returned to the absorber column completing the cycle.

### 49 *1.3 Novel contributions and outline of the paper*

50 This study focuses on the dynamic model development of the absorber of the chemical absorption plant. It offers what is  
51 thought to be a unique comparison of the accuracy of two approaches to modelling the absorption process– the  
52 equilibrium-based and rate-based approaches. Also dynamic analyses of some disturbances to the absorber performance  
53 were carried out. Two disturbances were considered:

- 54 • Decreasing flue gas flow supplied to the absorber from the upstream power plant, and
- 55 • Increasing the CO<sub>2</sub> loading of the lean MEA solution from the stripper of the capture facility.

56 A review of various approaches to modelling the chemical absorption process is described in section 2. Two approaches  
57 were compared – the equilibrium and rate-based approaches. The model development process was described in section 3.  
58 These models were validated with results from a pilot plant study [13] in section 4. Two dynamic scenarios were simulated

59 – reducing power plant load and increasing CO<sub>2</sub> loading of the lean solvent. The results are presented in section 5.  
60 Conclusions were drawn in section 6 and recommendations for future work were given in section 7.

## 61 **2. Developments in modelling chemical absorption of CO<sub>2</sub>**

62 Post combustion capture with MEA is a reactive absorption process. Two main phenomena are involved: mass transfer of  
63 CO<sub>2</sub> from the bulk vapour to the liquid solvent and the chemical reaction between CO<sub>2</sub> and the solvent.

64 A number of studies have employed steady state models of the chemical (or reactive) absorption process at different levels  
65 of complexity. Kenig et al describes the different levels of complexity of these models as illustrated in Figure 2 [14].

66 The equilibrium stage models assume theoretical stages in which liquid and vapour phases attain equilibrium. These  
67 models may assume the reactions are at equilibrium or may consider the reaction kinetics. The rate-based approach is more  
68 appropriate in modelling reactive absorption processes since phase equilibrium is hardly attained in practice. At its lowest  
69 level of complexity, the chemical reactions of the rate-based model are assumed to be at equilibrium. A more rigorous  
70 approach involves the inclusion of an enhancement factor to estimate actual absorption rates (with chemical reactions)  
71 from known physical absorption rates. The enhancement factor is calculated based on estimated reaction rates and is best  
72 suited for processes involving single irreversible reactions. This approach has been employed by a number of authors in  
73 developing steady state absorber and stripper models [15-17]. At the highest level available, reaction kinetics are modelled  
74 directly. Models consider mass transfer resistances, electrolyte thermodynamics, the reaction system as well as the column  
75 configurations and provide a direct estimation of concentration and temperature profiles by implementing reaction rates  
76 directly into the transport and balance equations in the film and the bulk of the fluid. This approach has been applied to a  
77 number of cases [10,14,18,19].

78 This study compares the equilibrium stage with the rate-based models both with reaction equilibrium (bottom and top left  
79 models in Figure 2).

80 The dynamic behaviour of the CO<sub>2</sub> absorption process for post combustion capture using MEA has not been extensively  
81 studied. Schneider et al considered the dynamic simulation of purification of coke plant gases [18]. Kvamsdal et al  
82 considered the dynamic simulation of only the absorber of the process using dynamic models of reduced complexity. The  
83 model employs an enhancement factor based on the assumption of pseudo first-order reaction regime. Kvamsdal et al  
84 adjusted both inlet flue gas flow rates and absorber heights to match pilot plant performance. In this study only the inlet  
85 flue gas flow rates to the absorber were adjusted. Kvamsdal et al also assumed a constant value for the heat of reaction and  
86 vaporization of water [9].

## 87 **3. Model development**

88 This section describes the model development of the absorber using the equilibrium- and rate-based approaches.

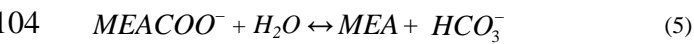
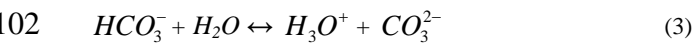
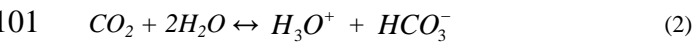
89 3.1. *Equilibrium-based approach*

90 The equilibrium-based approach was implemented in Aspen Plus<sup>1</sup> based on its Radfrac column model. This model was  
91 steady state and assumes theoretical stages in which liquid and vapour phases attain equilibrium and perfect mixing occurs.  
92 To describe non-equilibrium processes, the performance of each stage is adjusted using an efficiency correction factor  
93 [17,18]. For simulation purposes, the specifications presented in Table 1 were used. In section 4, all equilibrium based  
94 results were obtained from Aspen Plus.

95 The physical property method used is the Electrolyte Non-random-two-liquid (NRTL) model with electrolyte inserts for  
96 MEA. This insert includes new parameters and Henry's constant for CO<sub>2</sub> in MEA.

97 3.1.1. *Aspen Properties MEA solution chemistry*

98 MEA electrolyte solution chemistry is used to predict the equilibrium mass fractions in the liquid and vapour phases. The  
99 following are the set of equilibrium reactions describing this chemistry [20]:



105 3.2. *Rate-based approach*

106 In the rate-based approach, actual rates of multi-component mass and heat transfer as well as chemical reactions are  
107 considered directly [21]. The mass transfer is described using the two-film theory using the Maxwell Stefan formulation.  
108 Heat and mass transfer resistances are modelled in the liquid and vapour films.

109 The rate-based model was developed from the Gas-Liquid Contactor model in Process Systems Enterprise's Advanced  
110 Model Library using their process modelling tool, gPROMS. With gPROMS, accurate dynamic models of processes can be  
111 developed as it is equation-based and inherently dynamic.

112 3.2.1. *Model assumptions*

113 The following assumptions were used in developing this dynamic model:

- 114 • Plug flow regime  
115 • Linear pressure drop along the column  
116 • No accumulation in liquid and vapour films as well as bulk vapour

---

<sup>1</sup> Aspen Technology Inc.

- 117 • Phase equilibrium at interface between liquid and vapour films
- 118 • Negligible oxygen content in the flue gas
- 119 • Negligible solvent degradation
- 120 • Negligible heat loss to the surroundings
- 121 • Liquid phase reactions

122 3.2.2. Material and energy balances

123 Material and energy balances are carried out on the bulk liquid and vapour.

124 Bulk Liquid:  $\frac{dM_i}{dt} = \frac{-1}{L \cdot A} \frac{\partial F_i^L}{\partial y} + N_i \cdot Sp \cdot MW_i \cdot \omega$  (6)

125  $\frac{\partial F_i^L}{\partial y} \Big|_{y=1} = 0$  (7)

126 Where,

127  $M_i = x_i \times M, \quad i = 1, \dots, n$  (8)

128  $\sum_{i=1}^n x_i = 1$  (9)

129  $y$  is the axial position relative to the top of the absorber packing ranging from 0 (or top) to 1 (or bottom of the packing).

130  $\frac{dU}{dt} = \frac{-1}{L \cdot A} \frac{\partial F_H^L}{\partial y} + Sp \cdot \omega (H_{liq}^{cond} + H_{liq}^{conv} + H_{abs})$  (10)

131  $\frac{\partial T}{\partial y} \Big|_{y=1} = 0$  (11)

132 Where

133  $H_{abs} = N_{CO_2} \times h_{abs}$  (12)

134 The specific heat of absorption,  $h_{abs}$  (J/mol), is estimated as a function of temperature and CO<sub>2</sub> loading based on  
 135 expressions in literature [22].  $F_H^L$  is the liquid enthalpy flow rate (J/s).

136 Bulk Vapour:  $0 = \frac{-1}{L \cdot A} \frac{\partial F_i^V}{\partial y} - N_i \cdot Sp \cdot MW_i \cdot \omega$  (13)

137  $\frac{\partial F_i^V}{\partial y} \Big|_{y=1} = 0$  (14)

138  $0 = \frac{-1}{L \cdot A} \frac{\partial F_H^V}{\partial y} + Sp \cdot \omega (H_{vap}^{cond} + H_{vap}^{conv})$  (15)

139 3.2.3. Mass transfer

140 Mass transfer was modelled with resistances in the liquid and vapour films. The diffusivity ( $\chi$ ) of CO<sub>2</sub> in the liquid phase  
141 was based on expressions provided by Vaidya et al [23]. The diffusivity ( $\chi$ ) of CO<sub>2</sub> and other components in the vapour  
142 phase was estimated using the Fuller's equation [24]. Mass transfer coefficients in the liquid and vapour films were  
143 determined by correlations given by Onda et al [25]. Molar fluxes ( $N_i$ ) of each component were estimated using the  
144 Maxwell-Stefan formulation (applied to both liquid and vapour phases):

145 
$$\frac{1}{\delta} \frac{\partial x_i^M}{\partial z} = \frac{1}{c_t} \sum_{k=1}^n \left( \frac{x_i^M N_k - x_k^M N_i}{\chi_{i,k}} - \frac{\mu^R}{\mu} \frac{T}{298.15} \right) \quad (16)$$

146 Where,  $c_t$  is the total molar concentration in the phase,  $\delta$  is the film thickness and  $x_i^M$  is the molar fraction.

147 3.2.4. Physical properties

148 The physical property estimation models were set up in Aspen Properties. Through the CAPE-OPEN Thermo interface,  
149 gPROMS can take advantage of Aspen Properties' extensive physical property database. The Electrolyte-NRTL properties  
150 method was selected. For simplicity, only four main components were considered – MEA, water, carbon dioxide and  
151 nitrogen (oxygen content was incorporated into the nitrogen composition). Aspen properties also includes electrolyte  
152 inserts for the Electrolyte-NRTL property method where electrolyte solution chemistry is accounted for [20]. The same  
153 physical property model was used in the equilibrium- based model was used here as well.

154 MEA electrolyte solution chemistry is used to predict the equilibrium mass fractions in the liquid and vapour phases at the  
155 interface. The same set of equilibrium reactions described in equations (1-5) is used.

156 **4. Model validation**

157 The models developed were validated using data from the Separations Research Program at the University of Texas at  
158 Austin. The absorber column of the pilot plant is a packed column with a diameter of 0.427m and total height of 6.1m. This  
159 column consists of two 3.05m packed bed sections with a collector plate and redistributor between the beds [13]. Out of the  
160 48 experimental cases carried out in the research program, two cases (Cases 32 and 47) were selected for steady state  
161 validation purposes. These two cases were selected because of their relatively high and low liquid to gas (L/G) ratios  
162 respectively.

163 Table 2 shows the process conditions for the lean MEA and flue gas streams to the absorber while Table 3 shows some  
164 absorber column and packing specifications.

165 Simulation results were validated using the temperature profile of the absorber column measured in the pilot plant [13]. In  
166 addition the measured CO<sub>2</sub> loading of the amine solvent taken at different positions was compared with values obtained  
167 from simulation.

168 4.1 *Validation and comparison of equilibrium- and rate-based models*

169 4.1.1. *Case 47*

170 This case involved a relatively low liquid to gas (L/G) ratio thus a lower CO<sub>2</sub> capture level.

171 Because of the reported inaccuracy in the flue gas flow measurement [9,13], its value was adjusted to match reported  
172 capture levels as shown in Table 4. Both the equilibrium and rate-based models predicted lower rich solvent loading than  
173 what was measured while the absorption levels are virtually the same as measured.

174 The temperature profile in the absorber was used to validate the two models as shown in Figure 4. The rate-based model  
175 gives a slightly better prediction of the temperature profile. The equilibrium-based model predicts generally lower  
176 temperatures than what was measured.

177 4.1.2. *Case 32*

178 This case involved a relatively high liquid to gas (L/G) ratio thus a high CO<sub>2</sub> capture level.

179 Both models showed poor prediction of the temperature profile in the absorber. However, with further reduction in the inlet  
180 flue gas rate to 0.11kg/s, better predictions were observed as shown in Figure 6. However, this change implies higher CO<sub>2</sub>  
181 capture levels than what was measured in the pilot plant (Table 5).

182 These discrepancies (as seen in Table 6) may be due to the assumption that the reactions between CO<sub>2</sub> and MEA are at  
183 equilibrium as calculated by the electrolyte solution chemistry. Kinetically controlled reactions may therefore provide  
184 better predictions of the trend. The rate-based model still gives a better prediction of the absorber temperature profile  
185 (Figure 6) compared to the equilibrium based model. The equilibrium-based model predicts higher temperatures than those  
186 measured in the pilot plant study.

187 **5. Dynamic analysis**

188 These analyses consider the effect of disturbances on the performance of the absorber. Two scenarios are considered:

- 189
- Reducing power plant load – as a mid-merit power plant, power generation would not be continuously at base-  
190 load level. In this scenario, a 50% reduction in power plant load occurs.
  - Increasing lean MEA solution loading – with disturbances in the stripper column operation, such as reduced  
191 reboiler duty, the CO<sub>2</sub> loading of the lean MEA supplied to the absorber may increase. This scenario involves a  
192 10% increase in lean loading.
- 193

194 5.1 *Reducing power plant load*

195 In this scenario, the upstream power plant load was reduced from base-load (100%) to 50% load. It was assumed that the  
196 flue gas flow rate decreases correspondingly and the changes in component composition are negligible. This scenario was  
197 applied to Case 32. Two cases were considered:

- 198 • Case-A: Change of flue gas flow rate without changing liquid (solvent) flow rate
- 199 • Case-B: Change of flue gas flow rate with corresponding decrease in liquid solvent rate to maintain CO<sub>2</sub> capture
- 200 level

201 The process was simulated with the base-load conditions (Case 32) for three minutes after which the above changes were  
202 implemented in ten minutes. Finally conditions were maintained for eight minutes.

203 The two cases are illustrated in Figures 7

#### 204 *5.1.1 Case-A*

205 From Figure 8, the 100s curve represents the profile before dropping load. The other curves show a trend of increasing  
206 absorption levels with time. Since the flue gas flow rate is ramped down with time while the solvent flow rate is constant,  
207 an increase in L/G ratio occurs.

208 Figure 9 shows the change in the CO<sub>2</sub> absorption level as the flue gas leaves the absorber with the L/G ratio. CO<sub>2</sub>  
209 absorption levels increase almost linearly with L/G ratio up to ratios of about 8.0. Afterwards, the rate of increase reduces.

210 There is also a significant change in the temperature profile in the absorber as seen in Figure 10. The location of the  
211 temperature bulge gradually shifts toward the bottom of the column. Temperature values generally reduce as less quantities  
212 of CO<sub>2</sub> are absorbed.

#### 213 *5.1.2 Case-B*

214 By reducing the lean solvent feed rate correspondingly (by 50%), roughly the same capture level and temperature profile  
215 (Figures 11 and 12) could be maintained through the period of change. This suggests that the absorption process is more  
216 sensitive to the L/G (liquid solvent to flue gas) ratio than their actual flow rates. Since the amount of steam required for  
217 regeneration corresponds to the amount of lean MEA circulated, the energy requirement of the stripper could be  
218 correspondingly reduced.

#### 219 *5.2 Increasing lean MEA solution loading*

220 This scenario was applied to Case 32 (process conditions in Table 2). Conditions were maintained for three minutes. Then  
221 the CO<sub>2</sub> loading of the lean solution was ramped up by 10% (from 0.279 to 0.3069) within three minutes. Finally,  
222 conditions were then maintained for 30 minutes to achieve steady state. This is illustrated in Figure 13.

223 With increased CO<sub>2</sub> loading of the lean MEA supplied to the absorber, the CO<sub>2</sub> absorption level (Figure 14) drops from  
224 94.4% to 85.5%. CO<sub>2</sub> absorption levels could be maintained by either increasing the flow rate of lean MEA solvent to the  
225 absorber or decreasing the CO<sub>2</sub> loading of the solvent. The latter can be achieved by either increasing the stripper's reboiler  
226 duty or adding fresh MEA solution from solvent makeup tanks. Increasing the total solvent flow rate by 10% only results



227 in a capture level of 92.3%. Figure 15 shows that the temperature profile in the column is also affected by this change. The  
228 temperature bulge moves towards the bottom of the column.

## 229 **6. Conclusions**

230 This paper presents a study of the CO<sub>2</sub> capture with MEA based on the dynamic modelling of the process. Two models  
231 (equilibrium- and rate-based models) have been developed and compared. The rate-based approach yielded better  
232 predictions compared with the equilibrium-based approach.

233 Dynamic analyses of dropping the upstream power plant load and the effect of increasing CO<sub>2</sub> loading in the lean solvent  
234 were carried out. Simulation results reveal that the absorber operation is more sensitive to the L/G ratio than the actual flow  
235 rates of the solvent and the flue gas. Increased CO<sub>2</sub> loading in the lean solvent resulted in significant reduction in absorber  
236 performance.

## 237 **7. Future work**

238 It has been shown that the rate-based mass transfer model improves the predictions of the absorption process compared to  
239 the equilibrium based model. Another rate controlling factor is the reaction chemistry. The kinetics of the chemical  
240 absorption process would be improved by replacing the set of equilibrium reactions in the interface by kinetic and  
241 equilibrium reactions in the liquid film (top right model in Figure 2). This should give a better prediction of the absorption  
242 rates.

243 The stripper column model would subsequently be developed and the entire CO<sub>2</sub> capture facility model would be linked to  
244 a coal-fired power plant model for whole plant analyses.

## 245 **References**

246 [1] Freund P. Making deep reductions in CO<sub>2</sub> emissions from coal-fired power plant using capture and storage of CO<sub>2</sub>.

247 Proc. Inst. Mech. Eng. Part A J. Power Eng. 2003;217(1):1-8.

248 [2] Chalmers H, Gibbins J. Initial evaluation of the impact of post-combustion capture of carbon dioxide on supercritical  
249 pulverised coal power plant part load performance. Fuel, 2007 9;86(14):2109-23.

250 [3] IEA GHG. The capture of carbon dioxide from fossil fuel fired power stations. 1993;IEA GHG/SR2.

251 [4] IPCC. IPCC special report on carbon dioxide capture and storage. 2005.

- 252 [5] Abu-Zahra MRM, Schneiders LHJ, Niederer JPM, Feron PHM, Versteeg GF. CO<sub>2</sub> capture from power plants: Part I. A  
253 parametric study of the technical performance based on monoethanolamine. *International Journal of Greenhouse Gas*  
254 *Control*, 2007 4;1(1):37-46.
- 255 [6] Aroonwilas A, Veawab A. Integration of CO<sub>2</sub> capture unit using single- and blended-amines into supercritical coal-  
256 fired power plants: Implications for emission and energy management. *International Journal of Greenhouse Gas Control*,  
257 2007 4;1(2):143-50.
- 258 [7] Davidson R. Post-combustion carbon capture from coal fired plants - solvent scrubbing. 2007;CCC/125.
- 259 [8] Davison J. Performance and costs of power plants with capture and storage of CO<sub>2</sub>. *Energy*, 2007 7;32(7):1163-76.
- 260 [9] Kvamsdal HM, Jakobsen JP, Hoff KA. Dynamic modeling and simulation of a CO<sub>2</sub> absorber column for post-  
261 combustion CO<sub>2</sub> capture. *Chemical Engineering and Processing*, 2008; doi:10.1016/j.cep.2008.03.002.
- 262 [10] Kucka L, Müller I, Kenig EY, Górak A. On the modelling and simulation of sour gas absorption by aqueous amine  
263 solutions. *Chemical Engineering Science*, 2003 8;58(16):3571-8.
- 264 [11] Mahajani VV, Joshi JB. Kinetics of reactions between carbon dioxide and alkanolamines. *Gas Separation &*  
265 *Purification*, 1988 6;2(2):50-64.
- 266 [12] Vaidya PD, Kenig EY. CO<sub>2</sub>-alkanolamine reaction kinetics: A review of recent studies. *Chemical Engineering and*  
267 *Technology* 2007;30(11):1467-74.
- 268 [13] E. Ross Dugas. Pilot plant study of carbon dioxide capture by aqueous monoethanolamine, M.S.E. Thesis, University  
269 of Texas at Austin; 2006.
- 270 [14] Kenig EY, Schneider R, Górak A. Reactive absorption: Optimal process design via optimal modelling. *Chemical*  
271 *Engineering Science*, 2001 1;56(2):343-50.
- 272 [15] Pintola T, Tontiwachukwuthikul P, Meisen A. Simulation of pilot plant and industrial CO<sub>2</sub> MEA absorbers. *Gas*  
273 *Separation & Purification* 1993;7(1):47-52.
- 274 [16] Alatiqi I, Sabri MF, Bouhamra W, Alper E. Steady-state rate-based modelling for CO<sub>2</sub>/amine absorption—desorption  
275 systems. *Gas Separation & Purification* 1994;8(1):3-11.

- 276 [17] Al-Baghli NA, Pruess SA, Yesavage VF, Selim MS. A rate-based model for the design of gas absorbers for the  
277 removal of CO<sub>2</sub> and H<sub>2</sub>S using aqueous solutions of MEA and DEA. *Fluid Phase Equilibria*, 2001 7/30;185(1-2):31-43.
- 278 [18] Schneider R, Kenig EY, Górak A. Dynamic Modelling of Reactive Absorption with the Maxwell-Stefan Approach.  
279 *Chemical Engineering Research and Design*, 1999 10;77(7):633-8.
- 280 [19] Schneider R, Sander F, Górak A. Dynamic simulation of industrial reactive absorption processes. *Chemical*  
281 *Engineering and Processing*, 2003 12;42(12):955-64.
- 282 [20] AspenTech. Rate-based model of the CO<sub>2</sub> capture process by MEA using Aspen Plus. 2008; Available at:  
283 <http://support.aspentech.com/>. Accessed May, 2008.
- 284 [21] Noeres C, Kenig EY, Górak A. Modelling of reactive separation processes: reactive absorption and reactive  
285 distillation. *Chemical Engineering and Processing*, 2003 3;42(3):157-78.
- 286 [22] B. A. Oyenakan. Modeling of Strippers for CO<sub>2</sub> capture by Aqueous Amines University of Texas at Austin; 2007.
- 287 [23] Vaidya PD, Mahajani VV. Kinetics of the Reaction of CO<sub>2</sub> with Aqueous Formulated Solution Containing  
288 Monoethanolamine, N-Methyl-2-pyrrolidone and Diethylene Glycol. *Ind. Eng. Chem. Res.* 2005;44(6):1868-73.
- 289 [24] Reid RC, Prausnitz JM, Sherwood TK. The properties of gases and liquids. Third ed. New York: McGraw-Hill; 1977.
- 290 [25] Onda K, Takeuchi H, Okumoto Y. Mass transfer coefficients between gas and liquid phases in packed columns.  
291 *Journal of Chemical Engineering of Japan* 1968;1(1):56-62.
- 292 [26] Kvamsdal HM, Rochelle GT. Effects of the temperature bulge in CO<sub>2</sub> absorption from flue gas by aqueous  
293 monoethanolamine. *Ind. Eng. Chem. Res.* 2008;47(3):867-75.

Table 1 Specifications for Equilibrium-based model

Description	Value
Number of equilibrium stages	7
Type of packing	IMTP
Packing material	Metal
Packing Dimension (m)	0.038
Packing height (m)	6.1
Condenser	None
Reboiler	None
Physical Property Method	Electrolyte NRTL

Table 2 Process conditions for Cases 32 and 47

Stream ID	Case 47		Case 32	
	FLUE GAS	LEAN MEA	FLUE GAS	LEAN MEA
Temperature (K)	332.38	313.32	319.71	313.86
Pressure (10 <sup>5</sup> kPa)	1.033	1.703	1.035	1.703
Total flow (kg/s)	0.158	0.642	0.13	0.72
L/G ratio	4.6		6.5	
Mass-Fraction				
H <sub>2</sub> O	0.0193	0.6334	0.0148	0.6334
CO <sub>2</sub>	0.2415	0.0618	0.2520	0.0618
MEA	0	0.3048	0	0.3048
N <sub>2</sub>	0.7392	0	0.7332	0

Table 3 Absorber column and packing data

Description	Value
Column inside diameter (m)	0.427
Height of packing (m)	6.1
Nominal packing size (m)	0.0381
Specific area (m <sup>2</sup> )	145
Wetted area ratio	0.79

Table 4 Case 47 Process Conditions

	Pilot Plant	Equilibrium- Measurements based model	Rate-based model
Lean Solvent loading (mol/mol)	0.281	0.281	0.281
Rich Solvent loading (mol/mol)	0.539	0.500	0.487
CO <sub>2</sub> Absorption level (%)	69	68.8	69.2
Flue gas flow rate (kg/s)	0.158	0.172*	0.172*

\*Adjusted flue gas flow rate

Table 5 Case 32 Process Conditions

	Pilot Plant	Equilibrium- based model	Rate-based model
Lean Solvent loading mol/mol	0.279	0.279	0.279
Rich Solvent loading mol/mol	0.428	0.469	0.464
CO <sub>2</sub> Absorption level (%)	95	97.8	94.4
Flue gas flow rate (kg/s)	0.13	0.12*	0.12*

\*Adjusted flue gas flow rate



Table 6 Case 32 Process Conditions

	Pilot Plant	Equilibrium- Measurements based model	Rate-based model
Lean Solvent loading mol/mol	0.279	0.279	0.279
Rich Solvent loading mol/mol	0.428	0.456	0.456
CO <sub>2</sub> Absorption level (%)	95	99.6	99.5
Flue gas flow rate (kg/s)	0.13	0.11*	0.11*

\*Adjusted flue gas flow rate

## Nomenclature

$A$	Cross sectional area ( $\text{m}^2$ )
$c_t$	Total molar concentration ( $\text{mol}/\text{m}^3$ )
$F_i$	Component mass flow rate ( $\text{kg}/\text{s}$ )
$F_H$	Enthalpy flow rate ( $\text{J}/\text{s}$ )
$H$	Enthalpy ( $\text{J}$ )
$h$	Specific Enthalpy ( $\text{J}/\text{mol}$ )
$L$	Height of column ( $\text{m}$ )
$L/G$	Liquid to gas
$M$	Mass Holdup ( $\text{kg}/\text{m}^3$ )
$MW$	Molecular weight ( $\text{kg}/\text{mol}$ )
$N$	Molar flux ( $\text{mol}/\text{m}^2.\text{s}$ )
$n$	Number of components
$Sp$	Specific area ( $\text{m}^2/\text{m}^3$ )
$U$	Energy Holdup ( $\text{J}/\text{m}^3$ )
$x$	Mass fraction
$x_i^M$	Molar fraction
$y$	Axial position
$z'$	Film position

### Greek Symbols

$\delta$	Film thickness ( $\text{m}$ )
----------	-------------------------------

$\mu$	Viscosity ( $\text{Pa.s}$ )
$\omega$	Wetted area ratio
$\chi$	Diffusivity ( $\text{m}^2/\text{s}$ )

### Subscripts

$i$	Component number
$H$	enthalpy
$abs$	Absorption

### Superscripts

$L$	Liquid
$V$	Vapour
$Lf$	Liquid film
$Vf$	Vapour film
$Lb$	Liquid bulk
$Vb$	Vapour bulk
$cond$	Conduction
$conv$	Convection
$I$	Interface

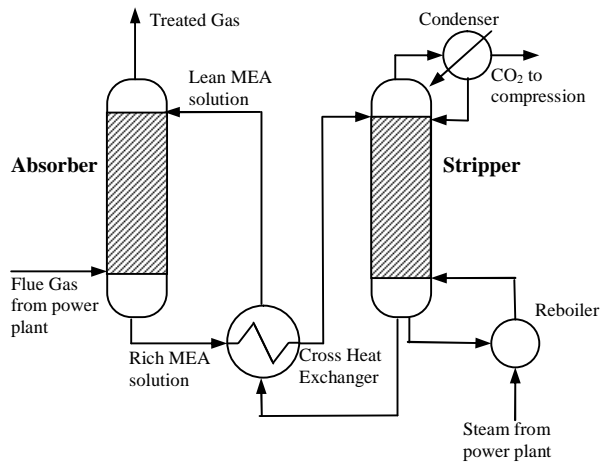


Figure 1 Simplified process flow diagram of Chemical Absorption process for post combustion capture from [9]

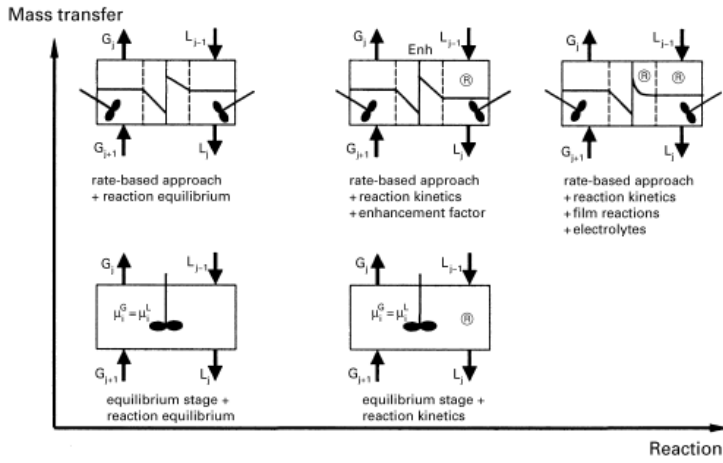


Figure 2 Different levels of reactive absorption model complexity from [14]

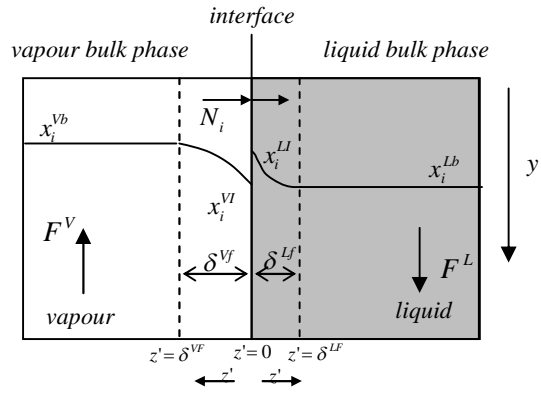


Figure 3 Liquid and vapour Bulks, films and interface adapted from [21]

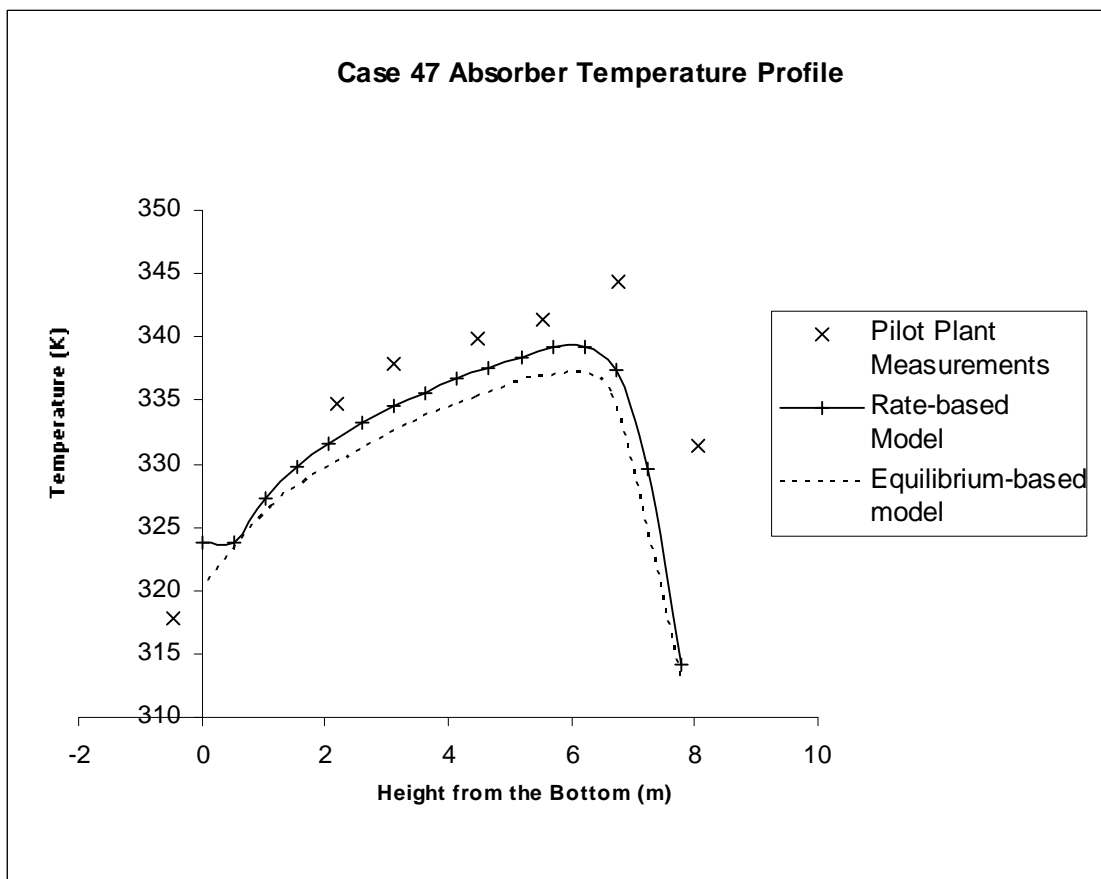


Figure 4 Absorber liquid temperature profile for case 47

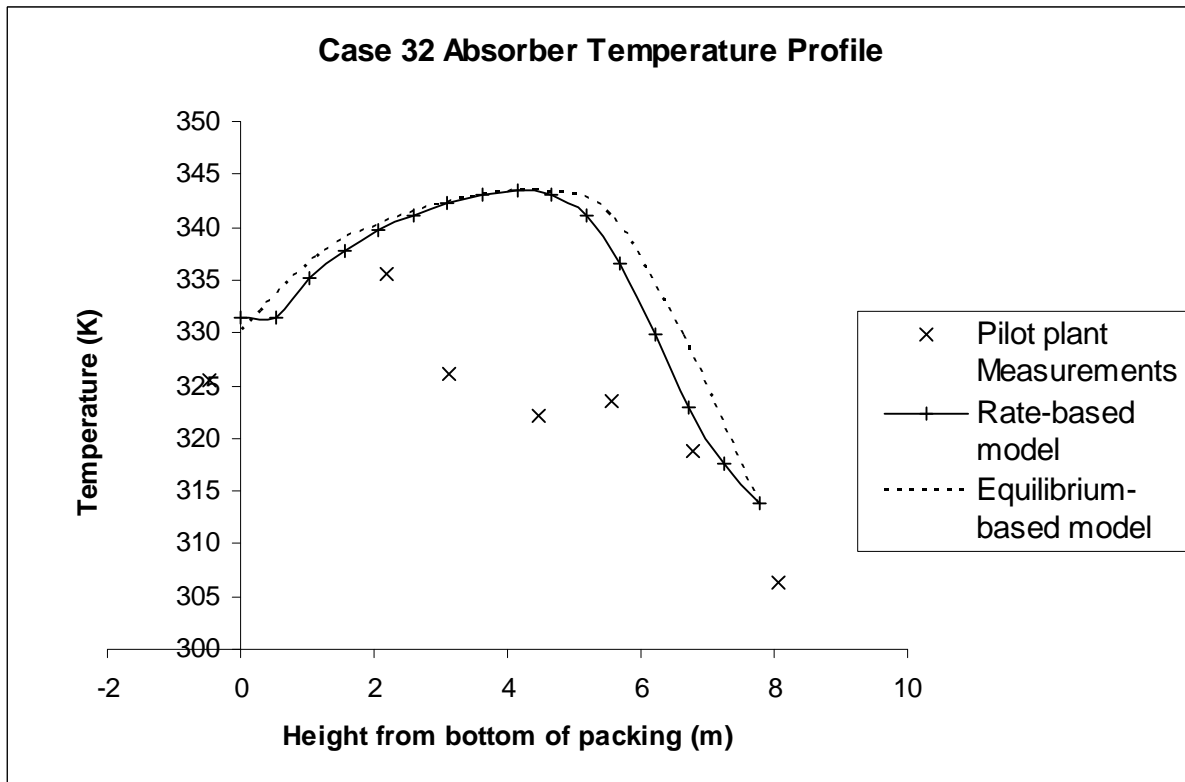


Figure 5 Absorber liquid temperature profile for case 32

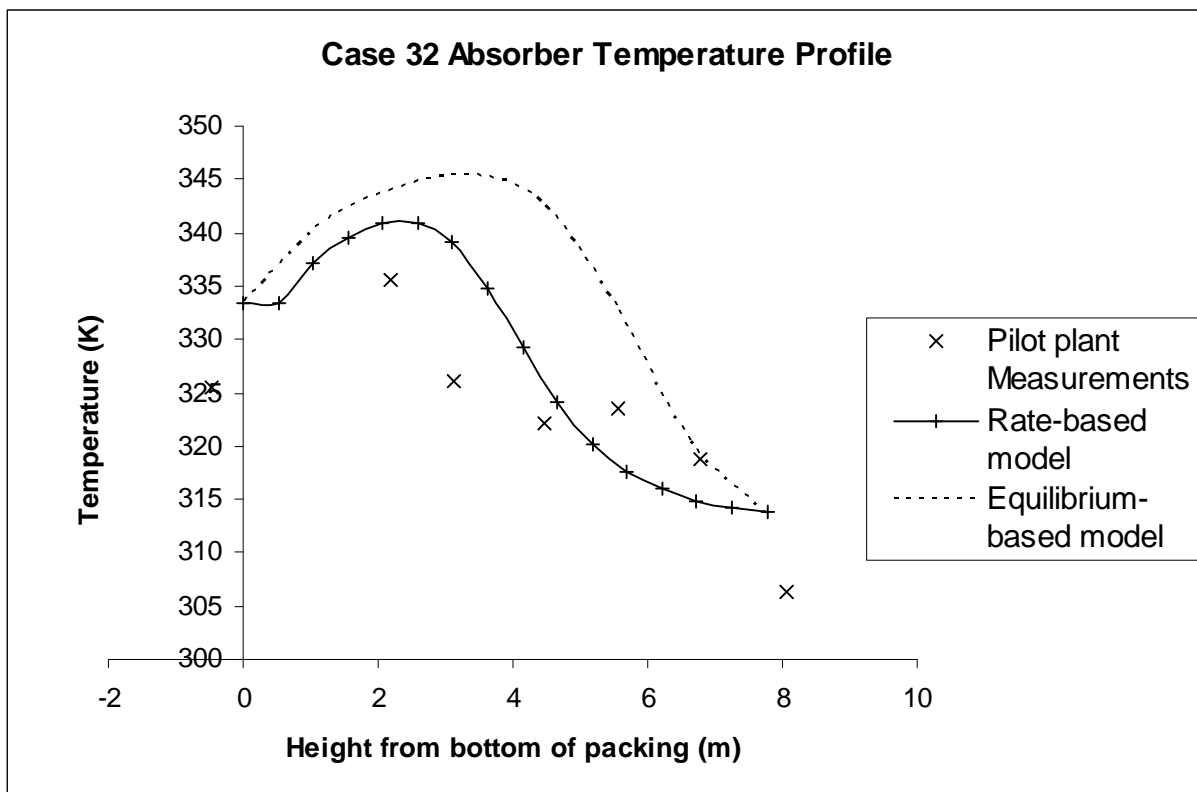


Figure 6 Absorber liquid temperature profile for case 32 with reduced flue gas flow



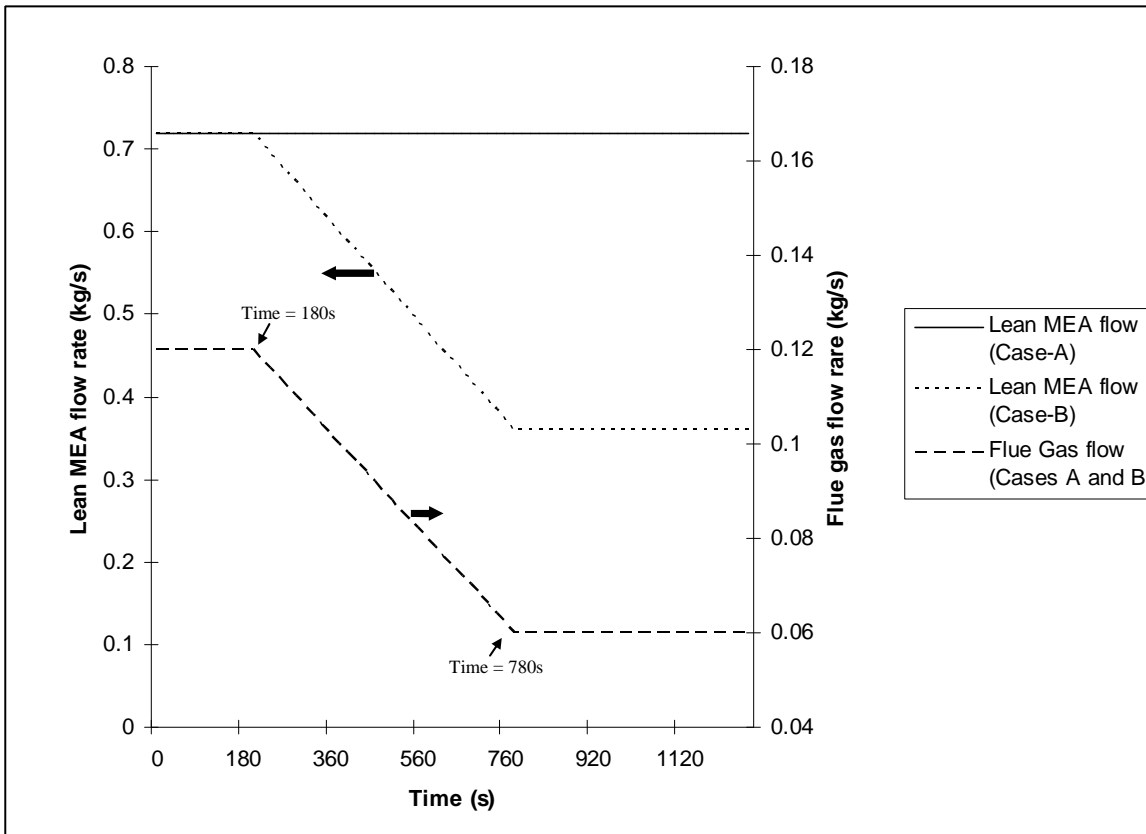


Figure 7 Flue gas and Lean MEA flow rate while reducing power plant load

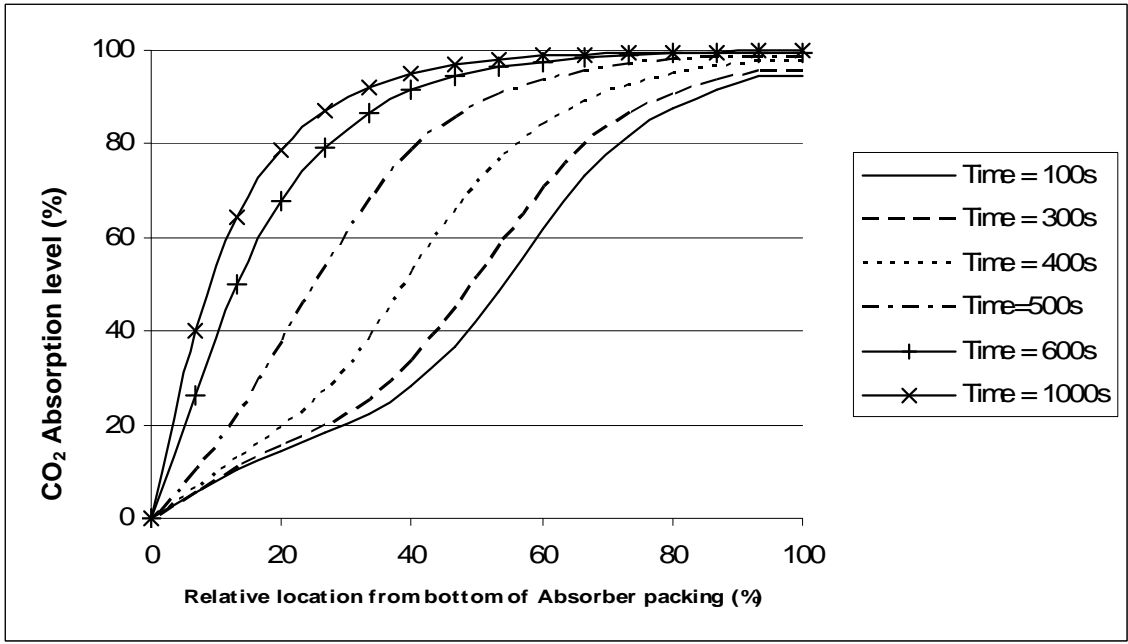


Figure 8 CO<sub>2</sub> absorption level – Case A

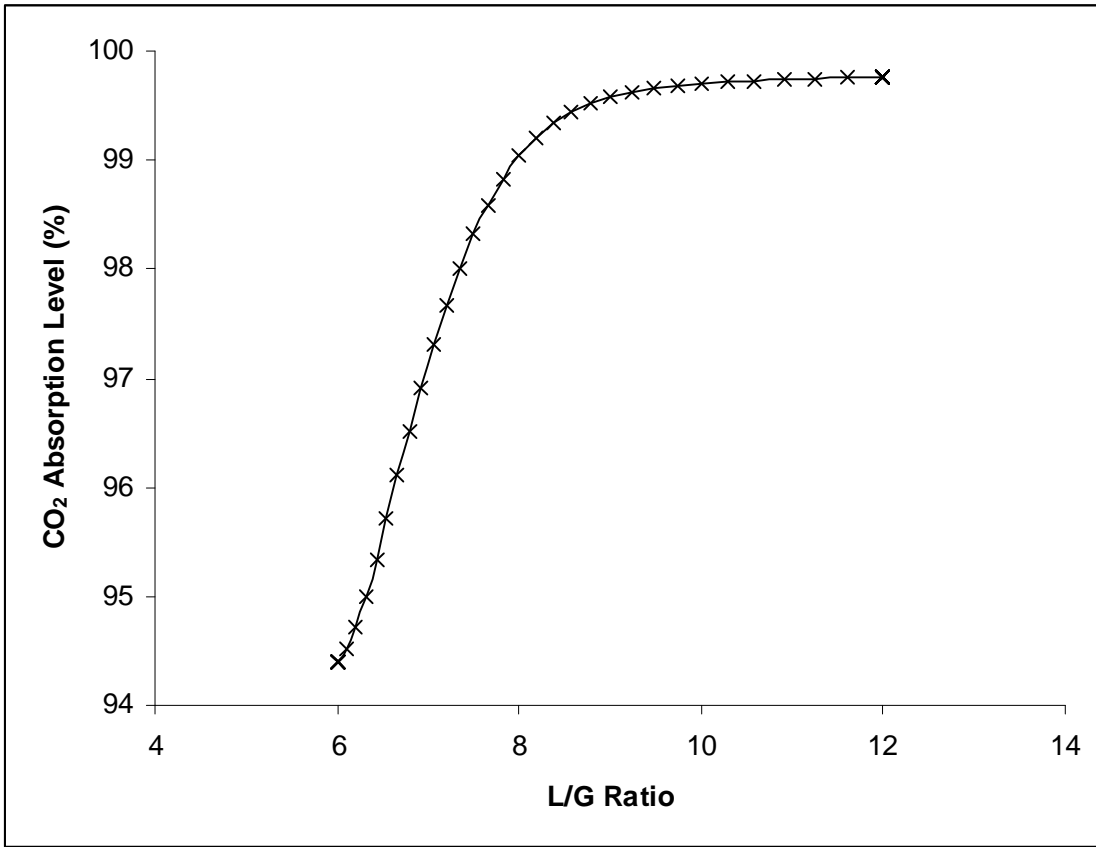


Figure 9 Change in CO<sub>2</sub> absorption levels with L/G ratio

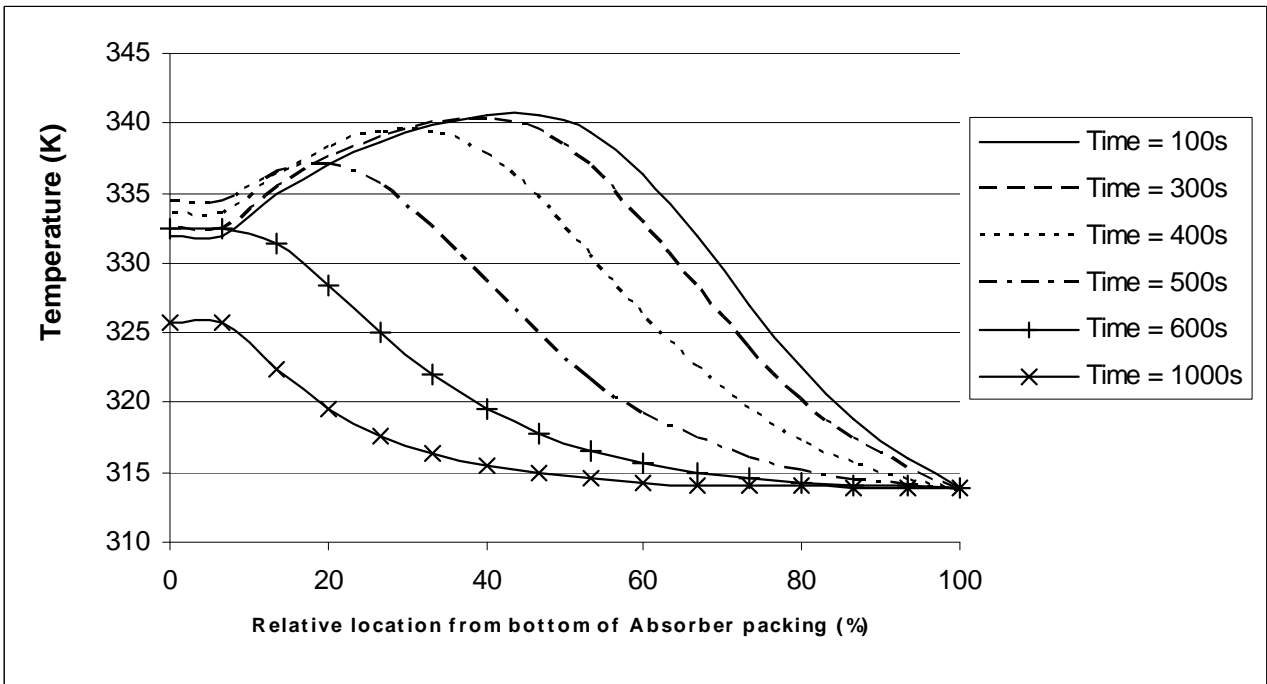


Figure 10 Temperature profile of absorber – Case A

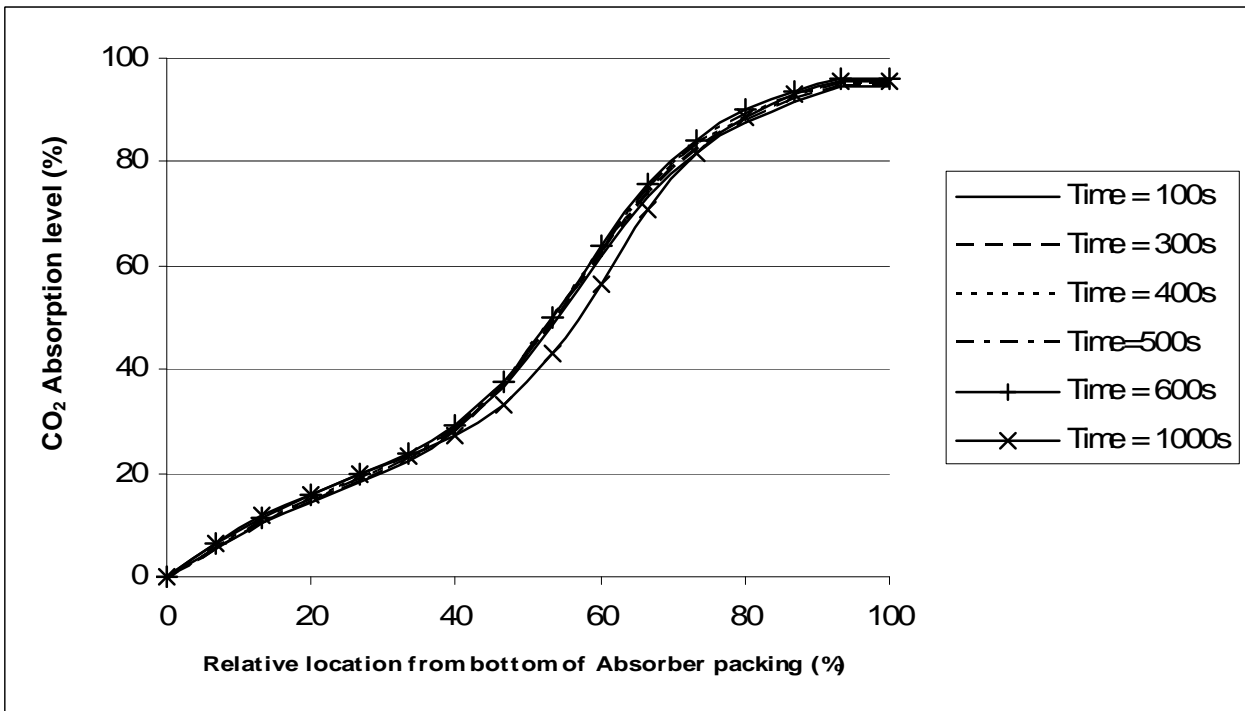


Figure 11 CO<sub>2</sub> absorption level – Case B

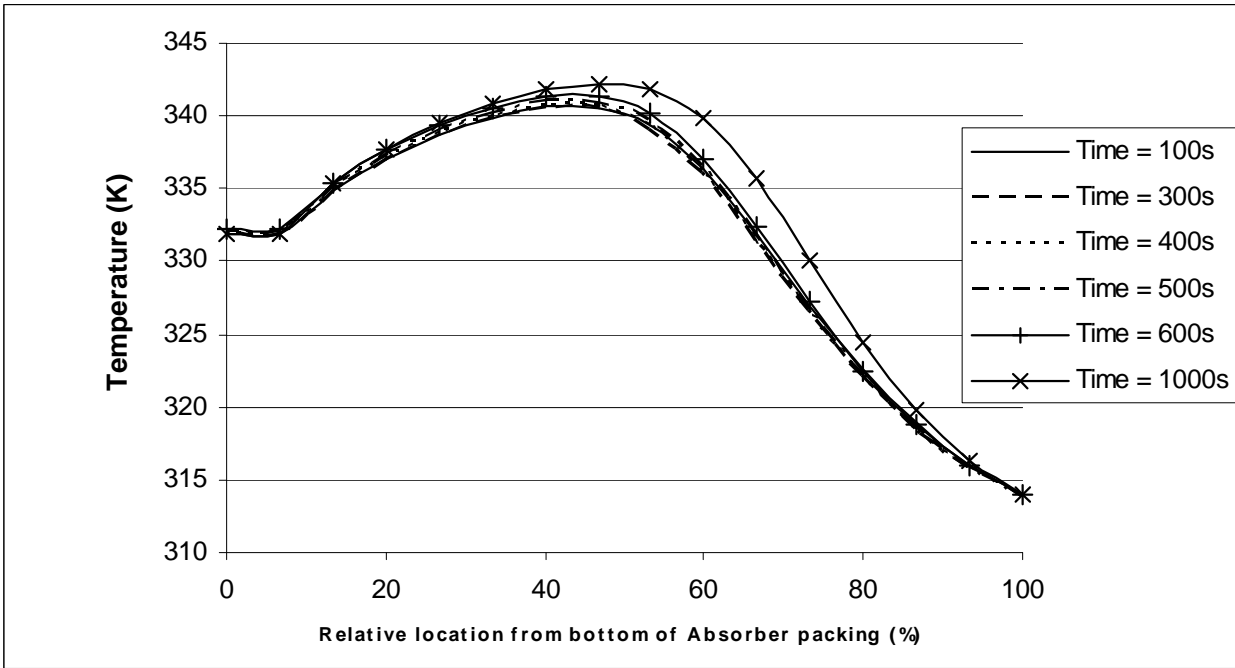


Figure 12 Temperature profile of absorber – Case B

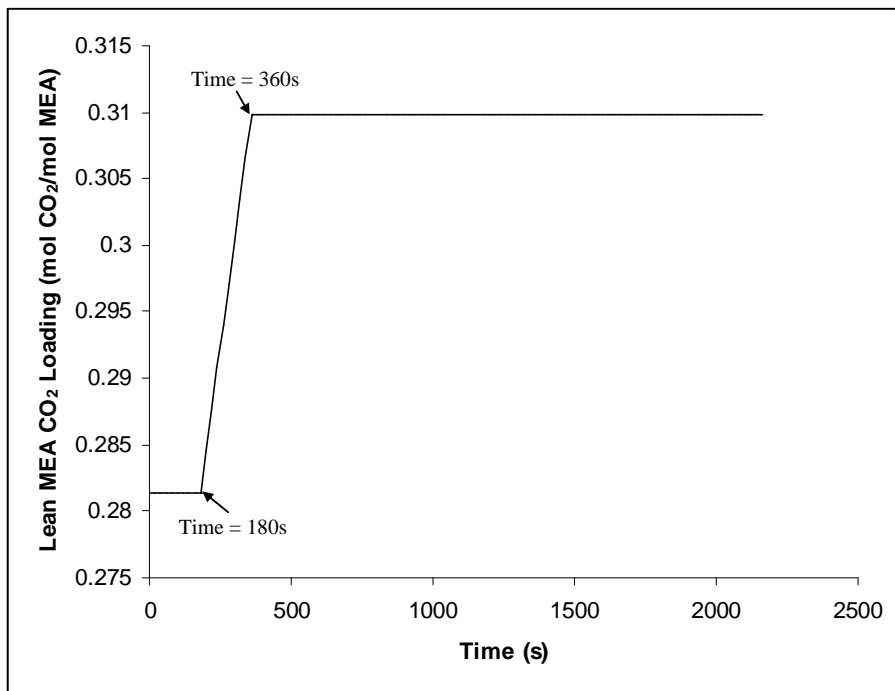


Figure 13 Increasing lean MEA CO<sub>2</sub> loading

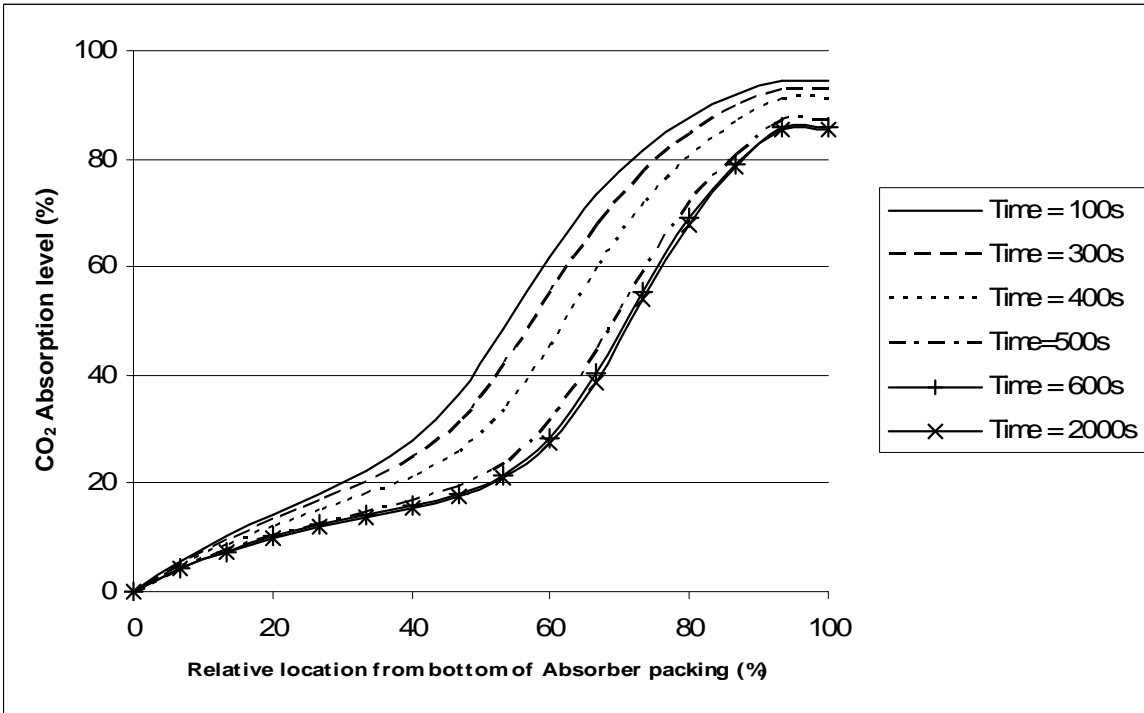


Figure 14 CO<sub>2</sub> absorption level while increasing CO<sub>2</sub> loading of lean MEA



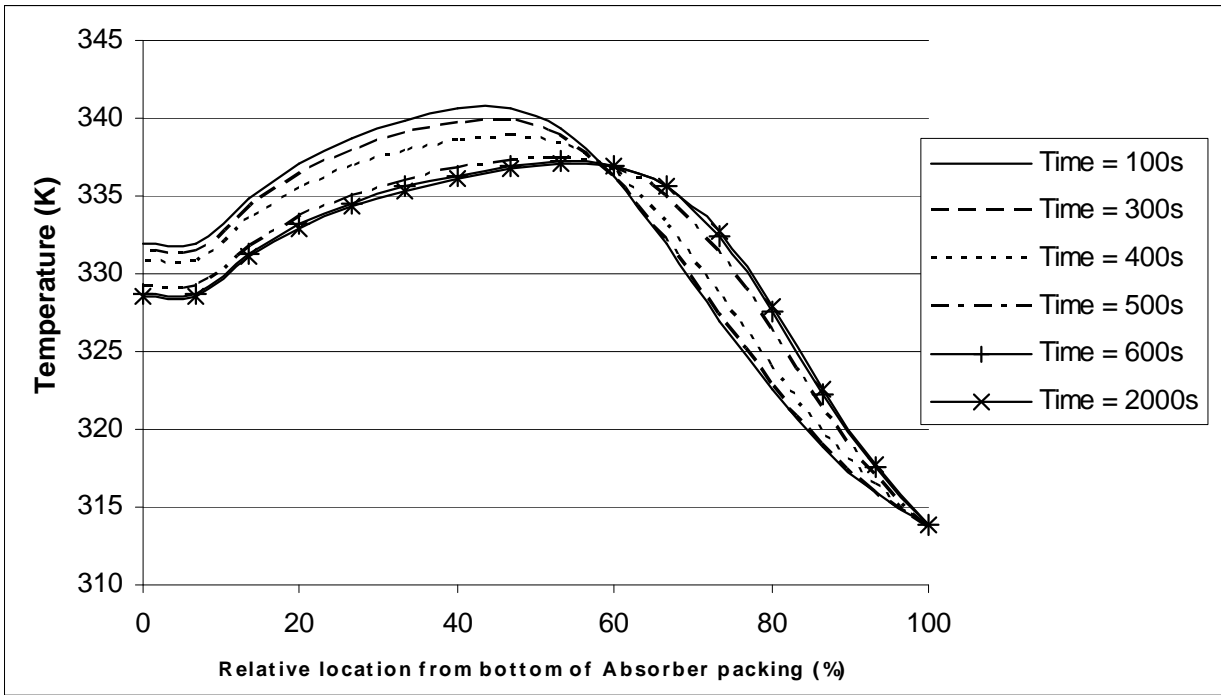


Figure 15 Temperature profile of absorber while increasing CO<sub>2</sub> loading of lean MEA